Computers and Chemical Engineering 153 (2021) 107422

Contents lists available at ScienceDirect

Computers and Chemical Engineering

journal homepage: www.elsevier.com/locate/compchemeng

Integrated design of biopharmaceutical manufacturing processes: Operation modes and process configurations for monoclonal antibody production

Sara Badr[a], Kozue Okamura[a], Nozomi Takahashi[a], Vera Ubbenjans[a,b], Haruku Shirahata[a], Hirokazu Sugiyama[a,*]

[a] Department of Chemical System Engineering, The University of Tokyo, 7-3-1 Hongo, Bunkyo-ku, 113-8656, Tokyo, Japan
[b] Faculty of Mechanical Engineering, RWTH Aachen University, Kackertstraße 9, 52072 Aachen, Germany

ARTICLE INFO

Article history:
Received 23 December 2020
Revised 30 April 2021
Accepted 21 June 2021
Available online 4 July 2021

Keywords:
Chinese hamster ovary cells (CHO)
kinetic model
perfusion cultivation
Periodic counter current (PCC)
chromatography
Continuous manufacturing
Techno-economic assessment

ABSTRACT

Monoclonal antibodies are leading the growing biopharmaceutical markets. To sustain the increasing demand, manufacturing processes should be optimized to increase efficiency and flexibility. This work investigates the impacts of the application of single-use equipment in batch, continuous, and hybrid scenarios. Operating costs and time are compared at different production scales from clinical to commercial manufacturing for individual unit operations and for the final integrated scenarios. A modified kinetic model is presented for the main cultivation unit. The model is validated using experimental data from literature and from a pilot facility using Chinese hamster ovary cells. Integrated scenarios with fed-batch cultivation and continuous capture have the lowest operating costs. The selection of operating modes across production scales is discussed along with further considerations for the design of integrated processes. The presented models could be used for the development of process design, control, and scheduling efforts for achieving sustainable biopharmaceutical manufacturing.

1. Introduction

Biopharmaceuticals represent a significant and growing share of the pharmaceutical market (Moorkens et al., 2017). They are being increasingly used for a broad range of diseases including cancer and autoimmune diseases with higher efficacy and lower side effects than traditional drugs (Kesik-Brodacka, 2018). In addition to 45 individual products as blockbusters in 2017, biopharmaceuticals also represent 40% of the products in clinical development globally, suggesting that the trends of growth in approvals and market share will continue in the next few years (Walsh, 2018). Monoclonal antibodies (mAbs) are the leading examples of biopharmaceuticals representing six of the top ten best selling drugs in 2018 (Walsh, 2018). Their market size is expected to continue expanding to almost 200 billion USD in 2022 (Grilo and Mantalaris, 2019). The expansion rate in the market size and number of products is not matched by an equal increase in production facilities, leading to a critical issue with the availability of biomanufacturing capacity (Seymour and Ecker, 2017). Conventional production processes are complex and lengthy. Therefore, to keep up with the increasing demand, as well as fend off competition from emerging biosimilars, manufacturing processes should be optimized to increase production flexibility and lower costs.

A standard process for mAb production includes upstream cell cultivation units followed by harvesting steps and downstream purification units to achieve the required product profile as shown in Fig. 1. Typically, biopharmaceutical production is conducted in batch mode with fed-batch cultivation operations followed by batch chromatography and filtration operations. There are simultaneous efforts undertaken to increase process efficiency and lower costs across drug substance and product manufacturing operations. These efforts range from cell line modifications to adjustment of culture media, operating conditions, and process configurations (Baumann and Hubbuch, 2017; Radhakrishnan et al., 2018; Zydney, 2016).

Two major changes attracting academic and industrial attention are the shifts to continuous manufacturing and single-use technologies (Lalor et al., 2019). The shift to continuous operations promises improved quality and homogeneity, as well as much higher levels of productivity and production flexibility with smaller equipment sizes (Fisher et al., 2019; Karst et al., 2018; Walther et al., 2019). Perfusion cultivation has already shown

* Corresponding author at: The University of Tokyo, 7-3-1 Hongo, Bunkyo-ku, Tokyo, 113-8656 Japan.
E-mail address: sugiyama@chemsys.t.u-tokyo.ac.jp (H. Sugiyama).

https://doi.org/10.1016/j.compchemeng.2021.107422
0098-1354/

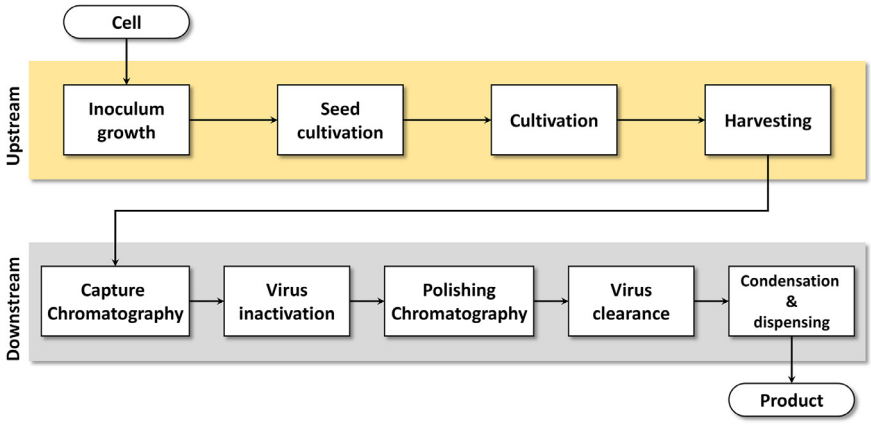

Fig. 1. Typical upstream and downstream drug substance manufacturing processes for monoclonal antibodies.

significant improvement in product titer, a trend which is expected to continue with titers reaching 3–5 g/L (Lin et al., 2017). This promises an even bigger productivity boost, which might shift the production bottleneck to downstream operations. Although integrated continuous operations have been demonstrated (Godawat et al., 2015; Warikoo et al., 2012), continuous operation in downstream units is not as mature as upstream with limited industrial applications (Hong et al., 2018; Papathanasiou and Kontoravdi, 2020). Measures, such as intermediate surge tanks, among others, are required for facilitating the integration of continuous or hybrid operations (Rathore et al., 2018). The introduction of continuous operations and the consequent utilization of smaller equipment also allows for wider implementation of single-use equipment, where reactor volumes are limited to below 2000 L. The use of single-use equipment allows for savings in water and energy associated with changeover cleaning operations, while reducing the risks of cross-contamination. Additionally, they allow for faster transitions between production cycles and higher production flexibility (Lalor et al., 2019; Rathore et al., 2018). The introduction of such trends could however, still introduce additional concerns. In the case of continuous operations, there could be additional operational problems in terms of increased clogging or problems related to maintaining sterility and cell aging (Croughan et al., 2015; Pollock et al., 2017). The use of single-use equipment could also lead to increased supply risks and leachable contamination (Shirahata et al., 2019a; Zürcher et al., 2020).

Comparisons of different operation modes and equipment have been conducted at different scales. For example, batch and continuous operations have been compared in terms of quality and productivity (Karst et al., 2018; Xu et al., 2017). Process simulation has been used to compare the economic and environmental performance of continuous, batch, and hybrid operations at multiple scales (Cataldo et al., 2020; Pleitt et al., 2019; Pollock et al., 2013a; Yang et al., 2019b). Preferable modes seemed to vary according to the production scale. For example, Bunnak et al. (2016) showed that the cost of goods for fed-batch and perfusion operations to be almost the same at small production scales (28 kg/yr), while Klutz et al. (2016) showed a clear advantage for fed-batch at 200 kg/yr scales. Pollock et al. (2013b) demonstrated that there is a dependence on the harvesting technology employed and demonstrated a trade-off between economic benefits and the operational risks. Studies also showed a decrease in costs with production scale in integrated scenarios (Pollock et al., 2017; Yang et al., 2019a). Pollock et al. (2017) indicated that at smaller scales, equivalent to clinical trials, that fully continuous operations are favorable to batch. However, the results of Yang et al. (2019a) suggested that the continuous process is more economically attractive at all scales, albeit with the fed-batch process becoming more competitive at the larger commercial scales. This comparison did not account for the use of single-use equipment, which limits the available equipment sizes, but could lead to reduction in energy and utility costs.

Many techno-economic studies have relied on experimental and plant data, or on process simulators with simplified models (Shirahata et al., 2019b). Reviews for available models for cell cultivation and purification units are given by (Badr and Sugiyama, 2020; Sha et al., 2018). However, there is still a need for developing high-resolution kinetic models and integrating them into the process evaluation frameworks to achieve a more comprehensive perspective (Badr and Sugiyama, 2020). Such models could then become the building blocks for more rigorous efforts for process design, optimization, and control.

This work aims to address these issues by comparing batch and continuous operations using single-use equipment for mAb production processes at different scales ranging from clinical to commercial production. Two process units are chosen as the focus of this work: the main cultivation and capture chromatography units. These units represent the bottleneck operations in terms of overall production time and costs (Pollock et al., 2017; Yang et al., 2019a). A new kinetic model for the cultivation unit is presented. The model is validated using experimental data from literature and from a pilot facility in Japan using different Chinese hamster ovary (CHO) cells at different operating modes. Dynamic simulations of batch, continuous, and hybrid operations are used to compare different production scenarios in terms of production time and costs. A further discussion of risk factors and operational hurdles is also presented. Additionally, aspects related to the design of integrated processes and the required modeling and assessment framework are also given. The models and insights developed in this work can be used to enhance understanding of process dynamics and integrated in further applications of process design and control. An earlier version of this work was presented in the proceedings of the 30th European Symposium on Computer Aided Process Engineering (Badr et al., 2020).

2. Process modeling and simulation

2.1. Cultivation models

In this work, two cultivation modes are investigated: (1) The fed-batch mode, where nutrient levels are maintained by feeding throughout the production, thus enabling the extension of batch durations and cell viability, and (2) the perfusion mode, where the cultivation media is constantly fed to the reactor with the simultaneous removal of reactor output to achieve continuous flow. Fig. 2 shows a schematic of the fed-batch and perfusion reactors.

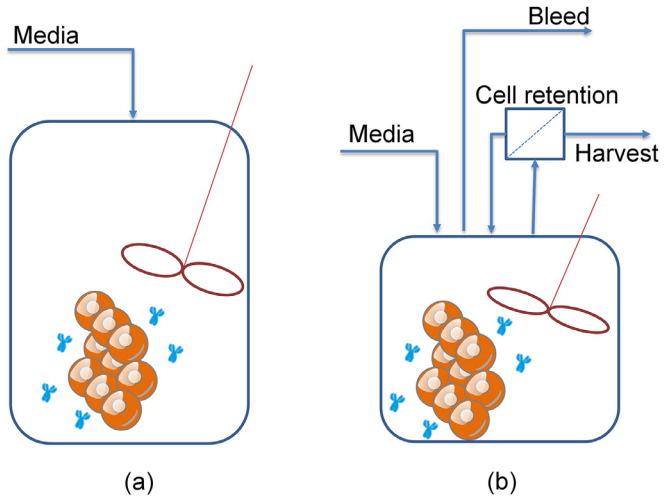

Fig. 2. Schematic of (a) fed-batch and (b) perfusion cultivation.

A model was developed based on previously presented literature models Kornecki and Strube, 2018; Xing et al., 2010). Previously published models had a poor fit to the experimental data obtained from the Kobe GMP consolidated lab facility in Japan (Manufacturing Technology Association of Biologics). Therefore, the set of model equations were modified to better reflect the experimental conditions and cell behavior at hand, especially concerning cell growth and death rates. Mass balance equations for key system components were developed with Monod type equations for cell growth and death rates, as shown in Eqs. (1-(7). Terms in bold are only valid for perfusion mode operations.

$$\frac{d(VX_V)}{dt} = (\mu - \mu_d)VX_V - \boldsymbol{F_{bleed}X_V} \tag{1}$$

$$\frac{d(VP)}{dt} = Q_P VX_V - (\boldsymbol{F_{harvest}} + \boldsymbol{F_{bleed}})\boldsymbol{P} \tag{2}$$

$$\frac{d(V[GLC])}{dt} = -\left(\frac{\mu - \mu_d}{Y_{X_V/glc}} + m_{glc}\right)VX_V + F_{in}c_{in} + F_{suppl}c_{suppl} - (\boldsymbol{F_{harvest}} + \boldsymbol{F_{bleed}})[\boldsymbol{GLC}] \tag{3}$$

$$\frac{d(V[LAC])}{dt} = Y_{lac/glc}VX_V - (\boldsymbol{F_{harvest}} + \boldsymbol{F_{bleed}})[\boldsymbol{LAC}] \tag{4}$$

$$\frac{d(V)}{dt} = F_{in} + F_{suppl} - (\boldsymbol{F_{harvest}} + \boldsymbol{F_{bleed}}) \tag{5}$$

$$\mu = \mu_{max}\left(\frac{[GLC]}{K_{glc} + [GLC]}\right)\left(\frac{KI_{lac}}{KI_{lac} + [LAC]}\right) \tag{6}$$

$$\mu_d = k_d\left(\frac{[LAC]}{KD_{lac} + [LAC]}\right)\left(\frac{KD_{glc}}{KD_{glc} + [GLC]}\right) \tag{7}$$

where, X_V is the viable cell density and V is the culture volume. F_{bleed}, $F_{harvest}$, F_{in}, and F_{suppl} are the bleed, harvest, main, and supplementary feed flows rates, respectively. P, $[GLC]$, and $[LAC]$ represent the antibody product, glucose and lactate concentrations, respectively. c_{in} and c_{suppl} are glucose concentrations in the main and supplementary feed streams, respectively. μ and μ_d are cell growth and death rates respectively, while μ_{max} and k_d are their corresponding maximum values. Q_P is the specific production rate. Y is the yield coefficient, where $Y_{x/y}$, for example, represents the change in the value of x with respect to variations in values of y. m_{glc} is the glucose maintenance coefficient. KI_{lac}, K_{glc}, KD_{lac}, KD_{glc} are the Monod model parameters representing the lactose and glucose half maximum rate concentrations for cell growth and cell death, respectively.

The model was validated using data from the Kobe GMP consolidated lab in Japan. Experiments for fed-batch mode were conducted using 50 L single-use bioreactors for a duration of 14 days using CHO-K1 cells. Experiments were conducted at 36.8 to 37.2 °C, at a stirring rate of 100 rpm. Basal media contained glucose at 7.4 g/L, while supplementary media was fed at 130 g/L. The culture was seeded from a solution of 0.32×10^6 cells/mL. Supplementary media was fed after 120 h once a day to maintain glucose concentrations at 3 g/L. Perfusion experiments were carried out using CHO-MK CL1001 cells for a duration of 31 days in a reactor of 2 L working volume. The culture was initiated with a solution of 0.56×10^6 cells/mL. An initial startup period of 6 days was carried out in batch mode before perfusion started. Glucose concentration in both base and feed media was at 7.4 g/L. Additional supplementary glucose at 450 g/L was also added to maintain the concentration at 2 ± 0.5 g/L in the culture liquid. An average perfusion rate of 1.4 vvd was carried out during the experiment. An alternating tangential flow (ATF) system was used for harvesting. Cell lysis and product losses during harvesting were not explicitly included in the model, but rather implicitly accounted for by fitting the model parameters to the experimental results after the harvest. The initial batch phase and subsequent growth and production phases were each modelled separately, as the model is insensitive to changes in cell metabolic behavior as a result of shifts in operating conditions. The model was further validated with experimental data from Xu and Chen (2016) and from Zhang et al. (2015). Zhang et al. (2015) employed a temperature downshift in the experiment, which has been shown to enhance productivity by inhibiting cell growth in perfusion cultures. To account for the temperature shift, the model was applied to three different phases in this experiment: the initial batch phase, the growth phase, and the production phase after the temperature shift. The initial batch phase in the Xu and Chen (2016) was not modelled, as insufficient data points were reported to reliably fit this region. Therefore, the model was applied only with the start of the perfusion operation on day 5 of the experiment.

2.2. Capture chromatography

The supernatant from the cultivation unit is sent to the capture chromatography unit, where the mAb product is adsorbed to the Protein A resin and is separated from most of the impurities such as host cell proteins (HCP)s and DNA. The column is operated in bind-elute mode, where the loading process involves the adsorption of the mAb onto the column. This is followed by a wash section to remove impurities from the column, then elution to release the mAb, and a regeneration phase for the column (cleaning in place (CIP) and equilibration). As such, the operation is batch in nature. To achieve continuous operation, multiple columns are operated in parallel, where one column or more are being loaded and the others are in the wash and elution phases. Prominent examples are the periodic counter-current chromatography (PCC) and simulated moving bed chromatography (SMB). The loading phase is the longest, therefore determining the duration of each cycle. Furthermore, some columns may be idle as loading is underway. Loading times can be further extended without risk of product loss in breakthrough by interconnecting the columns, thus increasing column utilization. Interconnecting the wash phase also helps to reduce product losses. A full description of the cycles in PCC operations is available in literature (Baur et al., 2016; Zydney, 2016). Fig. 3 shows one cycle of a 3 column PCC column.

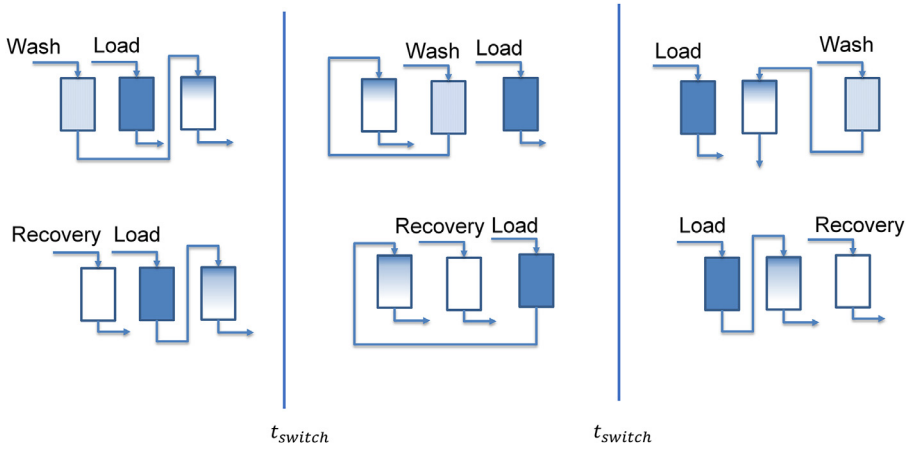

Fig. 3. Schematic representation of one cycle of 3-column PCC capture chromatography (Baur et al., 2016).

A shrinking core model was applied for the adsorption as previously introduced in literature Baur et al., 2016; Steinebach et al., 2016). The model addresses the issue, where adsorption on Protein A is very fast compared to the diffusion through the resin particles. Eqs. (8-(15) give the mass balance in the liquid phase in the column and in the resin particles:

$$\frac{\partial c}{\partial t} = \frac{u_{sf}}{\varepsilon_c}\frac{\partial c}{\partial x} + D_L\frac{\partial^2 c}{\partial x^2} - \frac{3}{r_p}\frac{1-\varepsilon_c}{\varepsilon_c}\varepsilon_p k_{tot}(c - c_p) \tag{8}$$

$$k_{tot} = \left(\frac{1}{k_f} + \frac{1}{k_s}\right)^{-1} \tag{9}$$

$$k_s = \frac{D(1-\alpha)^{1/3}}{1-(1-\alpha)^{1/3}} \tag{10}$$

$$\alpha = \frac{q_1}{q^{sat}}\frac{(1/K_D + c_{Feed})}{c_{Feed}} \tag{11}$$

$$k_f = \frac{1.09 u_{sf}}{\varepsilon_c} \tag{12}$$

$$\frac{\partial c_p}{\partial t} = \frac{3}{r_p}k_{tot}(c - c_p) - \frac{1-\varepsilon_p}{\varepsilon}\left(\frac{\partial q_1}{\partial t} + \frac{\partial q_2}{\partial t}\right) \tag{13}$$

$$\frac{\partial q_1}{\partial t} = k_{A1}\left[c_p\left(q^{sat} - q_1\right) - \frac{q_1}{K_D}\right] \tag{14}$$

$$\frac{\partial q_2}{\partial t} = k_{A2}\left[c_p(q_1 - q_2) - \frac{q_2}{K_D}\right] \tag{15}$$

where, c is the concentration of the bulk liquid phase, and c_p is the intra-particle liquid phase concentration. ε_c and ε_p are the column and particle porosity, respectively, while r_p is the particle radius. x is the distance travelled along the column length, and u_{sf} is the superficial velocity. D_L is the axial dispersion coefficient. k_{tot} is the total mass transfer coefficient, while k_f and k_s are the film and solid mass transfer coefficients, respectively. $q_1$and q_2 are the solid phase concentrations on the first and second adsorption sites, respectively. k_{A1} and k_{A2} are the adsorption rate constants at each site. α is the fraction of occupied adsorption sites, K_D is the equilibrium constant and q^{sat} is the saturation capacity of the resin. c_{Feed} is the feed concentration. A list of the parameters used in the simulation in this work is given in Table A1 in the Supporting Information. The boundary conditions are given by Eq. (16)

$$\begin{aligned} uc_{inlet} &= uc|_{x=0} - D_L\left.\frac{\partial c}{\partial x}\right|_{x=0} \\ \left.\frac{\partial c}{\partial x}\right|_{x=L} &= 0 \end{aligned} \tag{16}$$

where c_{inlet} is the column inlet concentration.

The model was discretized in space along the column length in finite volumes. The finite volume boundaries were smoothed by applying the weighed essentially non-oscillatory (WENO) method. A full description of the method is given elsewhere (von Lieres and Andersson, 2010). The resulting system of ordinary differential equations was then solved with the default *scipy.integrate.solve_ivp* solver with the BDF method in python.

2.3. Assessment

In this work, the model was used to create process simulations of individual and connected cultivation and capture chromatography units. Performance was assessed based on operating cost and time evaluations.

2.3.1. Processing time

The total operating time for fed-batch and perfusion runs are given by Eqs. (17) and (18), respectively:

$$t_{total,\ fed-batch} = N_{run}\left(t_{fed-batch} + t_{changeover}\right) \tag{17}$$

$$\begin{aligned} t_{total,\ perfusion} = {} & (N_{run} - 1)\left(t_{perfusion} + t_{empty} + t_{changeover}\right) + t_{demand} \\ & + t_{changeover} \end{aligned} \tag{18}$$

$$t_{empty} = \frac{V}{F_{harvest}} \tag{19}$$

where $t_{fed-batch}$ and $t_{perfusion}$ are the time to complete one run of fed-batch and perfusion operations and were taken in this work as 14, and 60 days, respectively. $t_{changeover}$ is the changeover time between runs and is taken as 1 day since the single-use equipment were assumed. N_{run} is the number of runs needed to fulfill the production demand. t_{empty} represents the time needed to empty the reactor after the feed has been stopped in perfusion runs. It was assumed that the harvest would continue at the same rate until the tank is empty. If a fraction of the 60 days is needed to comply with the required production amount in the perfusion run, then it was assumed that the run would stop if the required amount was reached and not continue to 60 days. t_{demand} is, thus, the time needed to fulfill the required production demand on the last run.

The operating time for batch capture chromatography is given by Eqs. (20-21) as the sum of loading, washing, elution, CIP, and equilibration times.

$$t_{total,\ batch} = n_{cycle}\left(t_{load} + t_{wash} + t_{elute} + t_{CIP} + t_{equil}\right) \tag{20}$$

Table 1
Column regeneration parameters for batch and PCC operations.

Parameter		Value
Linear velocity	$u_{sf,\ regen}$	300 cm h^{-1}
Buffer volume of wash (batch)	V_{wash}	6 CV
Buffer volume of elution	V_{elute}	5 CV
Buffer volume of CIP	V_{CIP}	5 CV
Buffer volume of column equilibration	V_{equil}	5 CV
Maximum Buffer volume of PLW (PCC)	$V_{PLW,\ max}$	2 CV
Buffer volume of post-load wash + wash (PCC)	$V_{PLW+wash}$	6 CV

CV= column volume, PLW= post-load wash.

$$n_{cycle} = \left\lceil \frac{V_{cult}}{Q\ t_{load}} \right\rceil \tag{21}$$

$$t_{load} = 0.7 \times t_{10\%} \tag{22}$$

$$\frac{c_{out}}{c_{in}} = 10\%\ @t = t_{10\%} \tag{23}$$

where n_{cycle} is the number of chromatography runs needed to treat all the input from the cultivation unit in one year. V_{cult} is the total cultivation volume to be treated and Q is the flowrate through the loading step of the chromatography. The loading time, t_{load}, was taken as a fraction of the time needed to reach 10% breakthrough, where the concentration in the liquid phase in the outlet is 10% of that in the inlet Eqs. (22) and ((23)). Table 1 presents the assumptions made for column regeneration based on the operation in the Kobe GMP consolidated lab. A regeneration surface velocity of 300 cm/h was assumed. Buffer solution volumes required for each step from wash to equilibration are given in Table 1. The time for each of the regeneration steps is thus given by Eq. (24), where S is the column surface area:

$$t_i = \frac{V_i}{u_{sf,regen} S},\ i \in \{wash, elute, CIP, equil\} \tag{24}$$

For a three-column PCC operation, there are three phases within each cycle, as shown in Fig. 3. Each phase consists of two configurations: one of batch loading, where one column is loaded, while the other two undergo an interconnected wash, and the other is of interconnected loading of two columns, while the third is being regenerated. Operation is switched at the end of each phase (t_{switch}), so that the second interconnected column becomes the batch loaded column. In this work, it was assumed that the switch occurs when the first interconnected column reaches 30% breakthrough inline with the experimental runs. A similar procedure was assumed for calculating the regeneration time of the column. In this case, the maximum buffer volume of the post-load wash (PLW), i.e., the interconnected wash, and for the total wash volume were assumed according to the values listed in Table 1. The time for PLW was assumed to be the same as the batch loading operation in that phase to avoid having idle columns. The total loading time was calculated according to the culture volume to be treated and the flowrate through the columns according to Eq. (25). The loading velocity was assumed to be smaller than the regeneration operations (<300 cm/h). It was thus assumed that column regeneration would occur completely during the loading time. The total process time was, hence, calculated according to Eq. (26) as the total loading time in addition to the regeneration time for the last cycle. The time for the batch loading phase was taken as the minimum of either the maximum PLW time and the time for 1% breakthrough according to Eq. (27):

$$t_{load,tot} = \frac{V_{\text{cult}}}{Q} \tag{25}$$

$$t_{total,\ PCC} = t_{load,tot} + t_{wash} + t_{elute} + t_{CIP} + t_{equil} \tag{26}$$

$$t_{load,\ batch} = \min\left(t_{PLW,max},\quad t_{1\%}\right) \tag{27}$$

2.3.2. Operating cost

The total operating cost for perfusion is given by Eq. (28) as the sum of the costs of media, utilities, single-use reactor bags, and labor. Eq. (29) gives the price of the bag (Yang et al., 2019b):

$$C_{cult\_operating} = C_{media} + C_{utilities} + C_{changeover} + C_{labor} \tag{28}$$

$$C_{changeover} = P_{bag}\left(V_r / V_{r\_ref}\right)^{0.75} \tag{29}$$

where V_{r_ref} is the reference reactor size of 50 L, P_{bag} is the price of the 50 L reactor, and V_r is the required reactor size. Table 2 presents the cost factors used for the cultivation process.

Operating costs for the chromatography were calculated according to Eq. (30) as the sum of the costs of mAb loss, buffer and resin consumption, and labor costs, which were calculated according to Eqs. (31-34)

$$C_{chrom\_operating} = C_{mAb,loss} + C_{buffer} + C_{resin} + C_{labor} \tag{30}$$

$$C_{mAb,loss} = \left(m_{loaded} - m_{purified}\right) \times P_{cultivation} \tag{31}$$

$$C_{buffer} = n_{cycle} u_{sf,regen} S \sum t_i P_{buffer,i} \tag{32}$$

$$for\quad batch\quad columns\quad i \in \{wash, elute, CIP, equil\},$$
$$for\ PCC\ columns\ i \in \{PLW + wash, elute, CIP, equil\}$$

$$C_{resin} = n_{col} V_{col} \frac{\left\lceil \frac{n_{cycle} Y_{resin}}{n_{life}} \right\rceil}{Y_{resin}} P_{resin} \tag{33}$$

$$C_{labor} = t_{total} P_{labor} N_{operator} \tag{34}$$

where m_{loaded} and $m_{purified}$ are the mass of the loaded and purified mAb, respectively. $P_{cultivation}$ is the upstream cultivation costs per gram mAb. In this work, if chromatography was modelled separately, an average value of 6400 JPY/g-mAb was assumed (1 USD≈100 JPY). In integrated scenarios, the actual cultivation costs were used instead. n_{col} and V_{col} are the column number and volume, respectively. Columns were assumed to be discarded after 200 cycles of loading and regenerations n_{life}, or when reaching its maximum lifespan Y_{resin}. Table 2 shows the most important cost parameters used for the calculation.

2.4. Dynamic simulations and integrated process scenarios

The developed models were first used to investigate the design of individual unit operations. The cultivation model was used to estimate variations in cost and production time of the two operating modes with changes in reactor volume and annual production scales. Fed-batch operation was assumed to be carried out using the CHO-K1 cell at conditions similar to those at the Kobe GMP consolidated lab in terms of feed media composition and operating conditions. The supplementary feeding rate was assumed as double that of the original experimental procedure after 120 h. Fitted model parameters (shown in Table 4) were used for the process simulation. Perfusion operation was assumed to be carried out at conditions similar to those reported by Xu and Chen (2016). Extension of the runs from 33 days in the reported experimental procedure to 60 days was assumed to be possible without significant changes in behavior. The concentration of the basal media was assumed to be 2 mM. Single-use equipment were assumed for all simulations. Scale-up effects were neglected in these simulations.

Table 2
Cost factors for cultivation and chromatography operating costs.

Cost item		Unit	Value	
Unit price for basal media	$P_{media,b}$	JPY L^{-1}	5000	
Unit price for supplementary feeding or perfusion media	$P_{media,f}$	JPY L^{-1}	10,000	
Unit price for electricity	$P_{electricity}$	JPY kWh^{-1}	14	
Power consumption of bioreactor	$e_{reactor}$	kW	1.5	
Price of a 50 L bag	P_{bag}	JPY bag^{-1}	30,000	
Hourly wage	P_{labor}	JPY h^{-1} $person^{-1}$	1250	
The number of operators	$N_{operator}$	person	Cultivation	2 (V_r <200 L) or 4 (V_r>200 L)
			Chromatography	4
Cost of resin	P_{resin}	JPY L^{-1}	1000,000	
Maximum number of cycles (resin)	n_{life}	–	200	
Lifespan of resin	Y_{resin}	yr	5	
Cost of PLW and wash buffer	$P_{buffer,PLW+wash}$ P_{wash}	JPY L^{-1}	58	
Cost of elution buffer	$P_{buffer,elute}$	JPY L^{-1}	21	
Cost of ClP buffer	$P_{buffer,ClP}$	JPY L^{-1}	13	
Cost of equilibration buffer	$P_{buffer,equil}$	JPY L^{-1}	58	
Cultivation operating cost	$P_{cultivation}$	JPY g-mAb^{-1}	$C_{cult\_operating}$ calculated @ integrated scenarios 6400 @ standalone chromatography scenarios	

*1 USD ≈ 100 JPY.

Table 3
Chromatography column sizes and parameters for individual unit and integrated process simulations.

Chromatography Mode	Inlet	Production scale [kg-mAb/yr]	Column diameter [cm]	Column length [cm]	Linear velocity [cm/h]
batch	Individual unit simulation @ (1 g/L, 3 g/L), and Integrated scenarios (Fed-batch, perfusion feed)	2	15	20	200
		50	40	20	200
		200	50	20	200
3-PCC	Individual unit simulation @ (1 g/L, 3 g/L), and Integrated scenarios (Fed-batch)	2	10	10	200
		50	30	20	200
		200	40	20	200
	Integrated scenarios (Perfusion)	2	7	10	200 *
		50	7	20	176.4 **
		200	14	20	176.1 **

* A surge tank is assumed between perfusion and PCC columns with 5 days pooling capacity.
** Velocity has been adjusted to match the inlet rate from the perfusion operation.

Operating costs and production time of chromatography operations were calculated for inlet mAb concentrations of 1 and 3 g/L at different production scales. A linear superficial velocity of 200 cm/h was assumed. For PCC continuous operations, 3 equal sized columns were assumed to be in operation. Table 3 shows the chosen column sizes and conditions for the chromatography simulations.

Integrated process scenarios were simulated at 2, 50, and 200 kg-mAb annual production scales. 200 working days were assumed to be available for manufacturing within a working year. The size of cultivation reactor was minimized to meet the demand within a working year. Maximum reactor sizes were assumed as 2000 L. In cases where it was not possible to achieve the required production amount within one reactor in a year, multiple reactors were assumed to be operated in parallel. The minimum size of equally sized reactors below 2000 L was chosen for such scenarios. The supernatant from the cultivation units was connected to the inlet of the chromatography units. Surge tanks were assumed for batch operation scenarios. Within scenarios of integrated perfusion and PCC columns, fully continuous operations were attempted whenever possible. To that end, the column superficial velocity in the 50, and 200 kg scale scenarios were adjusted to match the cultivation outlet. However, in the case of 2 kg production scales, full integration would not have been possible without the use of extremely small columns. In this case a surge tank was assumed, where the perfusion outlet is pooled for 5 days before being sent to the chromatography unit. Employed column sizes and superficial velocities for integrated scenarios are also listed in Table 3. In total, 12 integrated scenarios were assessed in this work, comparing fully continuous, fully batch, and hybrid operations of the cultivation and capture chromatography units at 3 different production scales. The manufacturing scales span those from clinical trials to full commercial production.

3. Results and discussion

3.1. Cultivation model validation

Fig. 4 shows the model fit to the CHO-K1 cell experimental run at the Kobe GMP consolidated lab in fed-batch mode for 14 days. Fig. 5 shows the model fit to the perfusion run using CHO-MK CL1001 cells at the Kobe GMP consolidated lab. Fig. 6 shows the model fit to previously published perfusion runs from Zhang et al. (2015) and from Xu and Chen (2016). The data for perfusion runs using the CHO-MK CL1001 cells and from Zhang et al. (2015) were fitted through different stages to account for changes in cell metabolism and behavior at different operating conditions and cell phases from growth to production. Data from Xu and Chen (2016) was only fitted after day 5 with the start of the perfusion due to lack of sufficient published data in the first days of experimental run. The fitted parameters for the CHO-K1 cell fed-batch, CHO-MK CL1001 cell perfusion, and Xu and

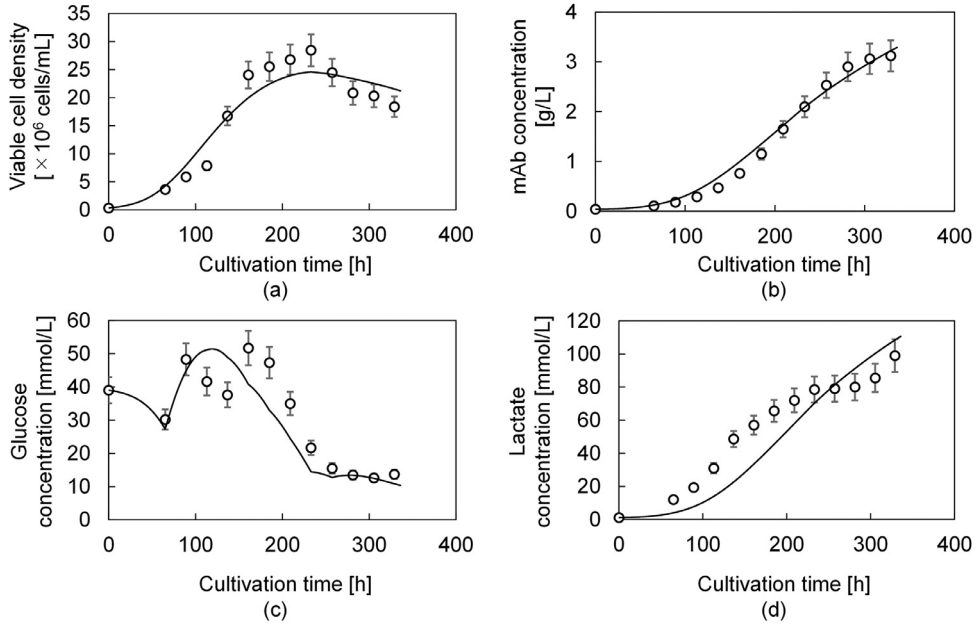

Fig. 4. Model validation for fed-batch operations using data from the 50 L scale CHO-K1 cell run at the Kobe GMP consolidated lab. Experimental points are shown with the standard measurement error. R^2 values are (a) 0.913, (b) 0.987, (c) 0.703, and (d) 0.757.

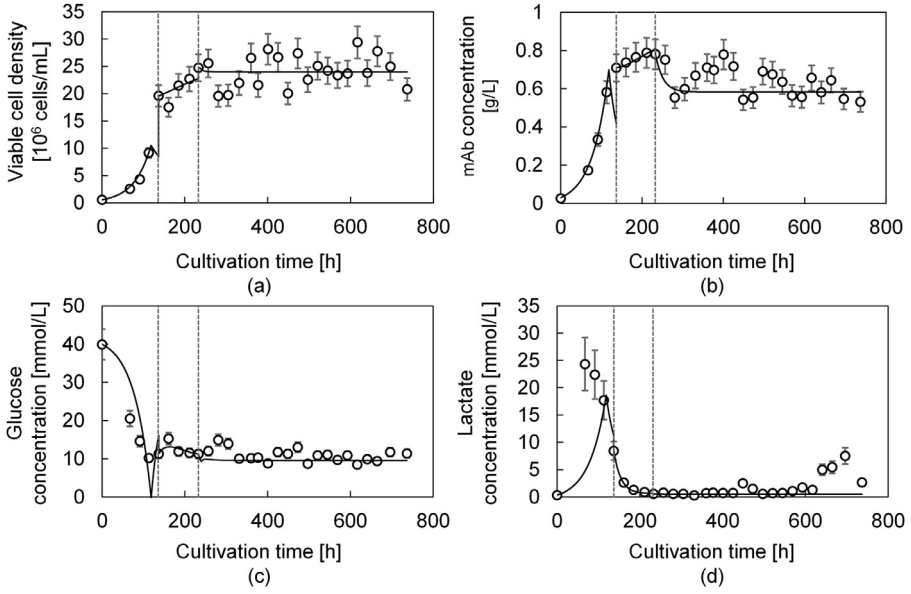

Fig. 5. Model validation for perfusion run using CHO-MK CL1001 cells at the Kobe GMP consolidated lab. The model was fitted separately to the initial batch phase (day 0–6), the growth phase (day 6–10), and the steady state perfusion phase (day 10–31). Experimental points are shown with the standard measurement error. Overall R^2, and RMSPE values are (a) 0.887, 11.9, (b) 0.823, 10.8, (c) 0.737, 20.2, and (d) 0.43, 52.0, respectively.

Chen (2016) perfusion runs are given in Table 4. Fitted parameters for Zhang et al. (2015) are given in Table A2 in the Supporting Information. Model parameters are system and cell-line dependent, where the fitted values of model parameters varied between cell lines, phases and operating modes. Some parameters were found to be negligible compared to other terms in the respective equations. However, trends could be seen which matched the understanding of the cell system. For example, the impact of cell death related terms (e.g. k_d, and KD_{glc}) on the four monitored concentrations (viable cell density, glucose, lactate, and mAb concentrations) was found to be relatively small, especially in perfusion runs. Furthermore, the average glucose concentration in the fed-batch run was higher than that in the perfusion, which led to a relatively smaller impact of the term K_{glc} on the growth rate term for the fed-batch run. The CHO-MK CL1001 cells are also known to be more sensitive to the presence of lactate at concentrations lower than 1 g/L, which is consistent with the more significant value of the KI_{lac} at the phase 3 in the perfusion with CHO-MK CL100 experiment compared to other phases. Another term that was found to be negligible for most runs, was the m_{glc}, which indicates that the energy spent for cell duplication was much higher than that used for cell maintenance. Overall, the model gave a good fit to the different experimental runs showing robustness with variations in cells and operating conditions. Trends for viable cell density and mAb production were very well described with the model for all four runs (Fig. 4 (a-b), 5 (a-b), and 6 (a-b), respectively). Fig. 6(b) features two axes for the mAb production to account for the differences in the reported data: the mAb titer (Xu and Chen, 2016), and the amount mAb produced (Zhang et al., 2015). The fitted parameter value for $Y_{lac/glc}$ (Table 4) was within the margin of er-

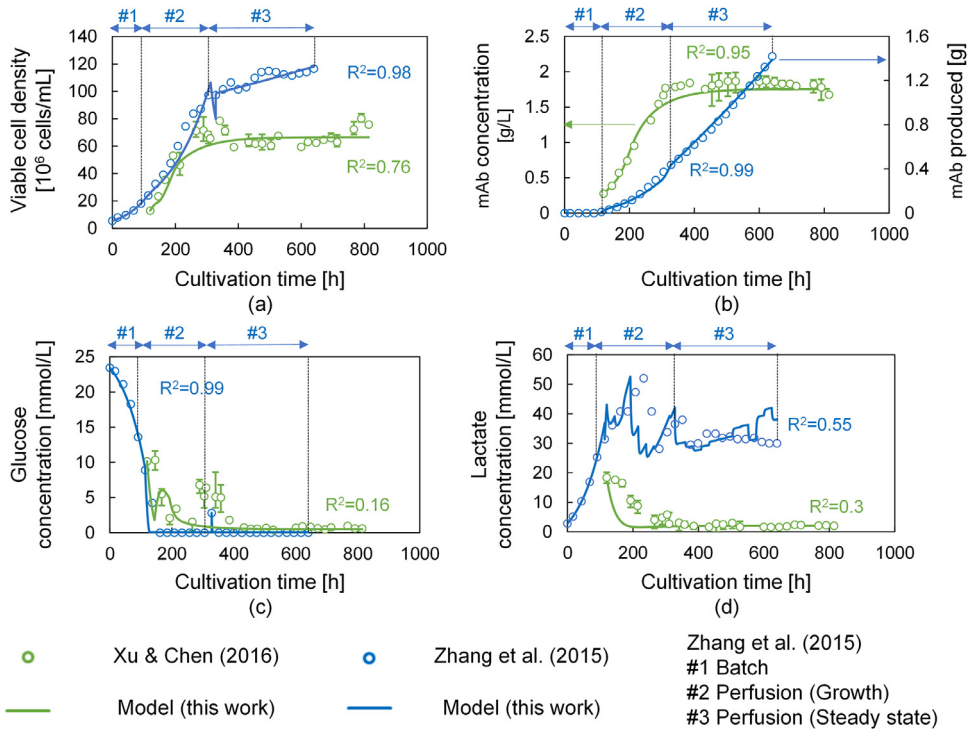

Fig. 6. Model validation with previously published experimental results from Xu and Chen (2016) and Zhang et al. (2015). A version of this figure was published in (Badr et al., 2020).

ror for the reported value obtained experimentally by the Xu and Chen (2016) of $1.25\times10^{-12}\pm$ 1.67 $\times$ 10^{-12} mmol/cell/h. Yet, the model still poorly described the changes in trends in lactate concentrations in the perfusion growth phase (Fig. 5(d), and 6 (d)). This is probably due to the changes in cell metabolism and shifting rates of lactate production and consumption by the cells. Lactate concentration within the fed-batch run (Fig. 4(d)) was relatively better described. This work aims to assess the productivity of the different operation modes. Therefore, the ability to accurately predict the mAb production amount is sufficient to achieve the purpose of the simulations. However, further improvements to the model to better describe the trends in cell metabolism and lactate concentrations would be important for future work aiming to simultaneously model productivity and quality aspects.

3.2. Simulation and assessment of individual units

Fig. 7 shows the simulation results of operation cost (Fig. 7 (a-c)) and time (Fig. 7 (d-f)) of the cultivation unit using different reactor volumes in fed-batch and perfusion modes. The results show the large gap in the expected productivities between the different modes, with perfusion highly outperforming fed-batch operation at all production scales and reactor volumes (Fig. 7 (d-f)). Even using the largest possible single-use reactor volume (2000 L), it would not be possible to produce 200 kg of mAb within one year; therefore multiple reactors must be used in parallel to fulfill the demand (Fig. 7(f)). The perfusion reactor of the same size, on the other hand, would be able to meet the required production within only 73 days. The cost of perfusion operation to produce the same amount of mAb is however, higher than fed-batch production at this scale (Fig. 7(c)). The assumption of two fed-batch reactors operating in parallel would yield the required amount within 248 days, with fed-batch still having the lower overall costs. Labor and utility costs are proportional to the operating time. Fig. 8 shows the breakdown of cultivation costs per gram mAb for fed-batch and perfusion operations at different reactor volumes and production amounts. At smaller reactor sizes, labor costs are a dominant cost factor for fed-batch operations due to the extended operating times (Fig. 7(d)). The impact of labor costs is normalized at larger reactor sizes and production scales. Fig. 8 shows that feed media is a major cost factor. Feed media consumption is linearly proportional to the production volume. The rate of change of cost with production capacity is almost equal at different reactor sizes. The rate of increase of media consumption with production scale is higher for perfusion operations than that of fed-batch. The feed media consumption, thus, represents the main cost element in perfusion operations. Perfusion operation has a cost advantage only at small production scales with small reactor volumes (Fig. 7(a)). At such small reactor volumes, the large difference in the processing times between fed-batch and perfusion operations leads to much higher labor cost for fed-batch operations compensating for the difference in media consumption for small production capacities. This pattern holds for reactor sizes smaller than 80 L. At larger reactor sizes, the increase in media costs for perfusion makes it the costlier option for the same production scale and reactor volume (Fig. 7 (b-c)). The length of individual runs was assumed as 60 days for perfusion and 14 days for fed-batch in this analysis. The length of production runs can vary in industrial operations, (e.g. 30 day perfusion runs). Varying the length of one run would primarily affect the number of changeover operations to achieve the desired production amount. Changeover mainly impacts operation time and the single-use bag reactor costs in this analysis. Changeover time was assumed as one day. Given the large difference between the required production time in fed-batch and perfusion, changeover time would thus be negligible in this comparison. Fig. 8 also shows that the cost of bag reactors is very small compared to the media and labor costs.

Fig. 9 shows the comparison of production cost and time per gram of purified mAb between batch and 3-column PCC capture at different production scales and inlet titers. Titers of 1 and 3 g/L correspond to typical values of perfusion and fed-batch upstream cultivation, respectively. Fig. 9(a) shows that chromatography costs

Table 4
Estimated Cultivation model parameters.

Parameter		Perfusion CHO-MK CL1001 cells Kobe GMP consolidated lab			Fed-batch CHO-K1 cells Kobe GMP consolidated lab.	Perfusion Xu and Chen (2016)
		Phase 1 (day 0–6)	Phase 2 (day 6–10)	Phase 3 (day 10–31)		(After Day 5)
K_{glc}	[mmol/L]	*	0.972±0.102	80.5±6.71	*	(4.83±0.244) ×10^{2}
KI_{lac}	[mmol/L]	*	*	(3.83±0.195) ×10^{-2}	7.10±0.07	*
KD_{lac}	[mmol/L]					
m_{glc}	[mmol/cell/h]	*	*	*	(82.3±1.06) ×10^{-12}	*
Q_p	[g/cell/h]	(1.66±0.34)× 10^{-12}	(2.10±0.107) ×10^{-12}	(1.40±0.106) ×10^{-12}	(8.18±0.173) ×10^{-13}	1.10×10^{-12} ± 9.60×10^{-14}
μ_{max}	[h^{-1}]	2.48×10^{-2} ± 6.17×10^{-4}	4.08×10^{-2}± 3.23×10^{-4}	4.86± 0.236	5.17×10^{-2}± 2.36×10^{-4}	1.54±0.109
k_d	[h^{-1}]	*	*	*	2.32×10^{-2}± 2.5×10^{-4}	*
$Y_{Xv/glc}$	[cell/mmol]	(2.48±0.21)× 10^{8}	(4.82±0.141) ×10^{8}	(4.06±0.208) ×10^{8}	1.33×10^{9}± 1.02×10^{7}	(2.25±0.162) ×10^{9}
$Y_{lac/glc}$	[mmol/cell/h]	(4.55±0.98)× 10^{-11}	(1.64±0.112) ×10^{-12}	(1.21±0.106) ×10^{-12}	2.76×10^{-11}± 4.76×10^{-13}	1.33×10^{-12} ± 8.37×10^{-14}
KD_{glc}	[mmol/L]	*	*	*	1.54± 0.034	*
Xv RMSPE	[–]	28.4	8.24	12.0	21.8	12.3
GLC RMSPE	[–]	40.2	7.06	16.0	20.9	53.4
LAC RMSPE	[–]	47.4	14.8	60.8	36.9	41.4
mAb RMSPE	[–]	19.4	1.97	12.1	22.5	6.36

* Terms shaded in gray indicate that the term is negligible relative to others in the respective equations.

per gram mAb purified decrease with the production scale. This is mainly due to the decrease in labor costs per gram. Labor costs are directly correlated to the production time. Fig. 9(b) shows the great reduction in processing time per gram purified from small scale production (2 kg) to large (200 kg). For both operation modes, the cost of resin per gram of mAb is lower at the higher scales because the columns can be used to their full capacity before being discarded. The cost of resin per gram of mAb is lower for PCC scenarios due to the higher column utilization enabled by the extended loading time without product loss in interconnected columns. The results in the Figure show that scenarios with batch columns had higher costs per gram mAb than PCC capture. When using the same column sizes, PCC operation should result in lower processing time than batch due to the parallel operation of column loading and regeneration. In this simulation, PCC columns were chosen to be smaller than the batch for the corresponding scenario (Table 3) to avoid excessively high resin costs. This resulted in longer processing times for PCC columns in the 1 g/L scenarios (Fig. 9(b)). In the 1 g/L scenarios, the inlet is assumed to originate from continuous perfusion cultivation, suggesting that upstream processes are the bottleneck regarding processing times and downstream operations are running in parallel. Therefore, prioritizing costs over time in downstream operations, in this case, is justified. In the 3 g/L scenarios, the processed volume is smaller than in the low inlet titer scenarios, thus resulting in lower loading time. In these scenarios, the simultaneous achievement of lower operating time and costs compared to the equivalent batch scenarios is possible.

3.3. Assessment of integrated scenarios

Table 5 shows the simulation details and results for integrated cultivation and capture scenarios, running in batch (FB-B), continuous (P-PCC), and hybrid (FB-PCC and P-B) modes at different annual production scales. Each scenario is described in terms of the number, and size of cultivation reactors, in addition to the resulting titer and the time needed for the capture step. All simulations assumed a working time of 200 days for the cultivation step. Large scale production of 200 kg/yr required more than one fed-batch reactor operating simultaneously to be completed within the set limit. Fig. 10 shows the results of the operating costs per gram mAb for the same scenarios. Overall, the hybrid scenario with fed-batch cultivation and continuous capture gave the lowest cost per gram mAb at all production scales. Differences in downstream yields and subsequent product losses led to slight variations in the required production amounts and the total costs. It is worth not-

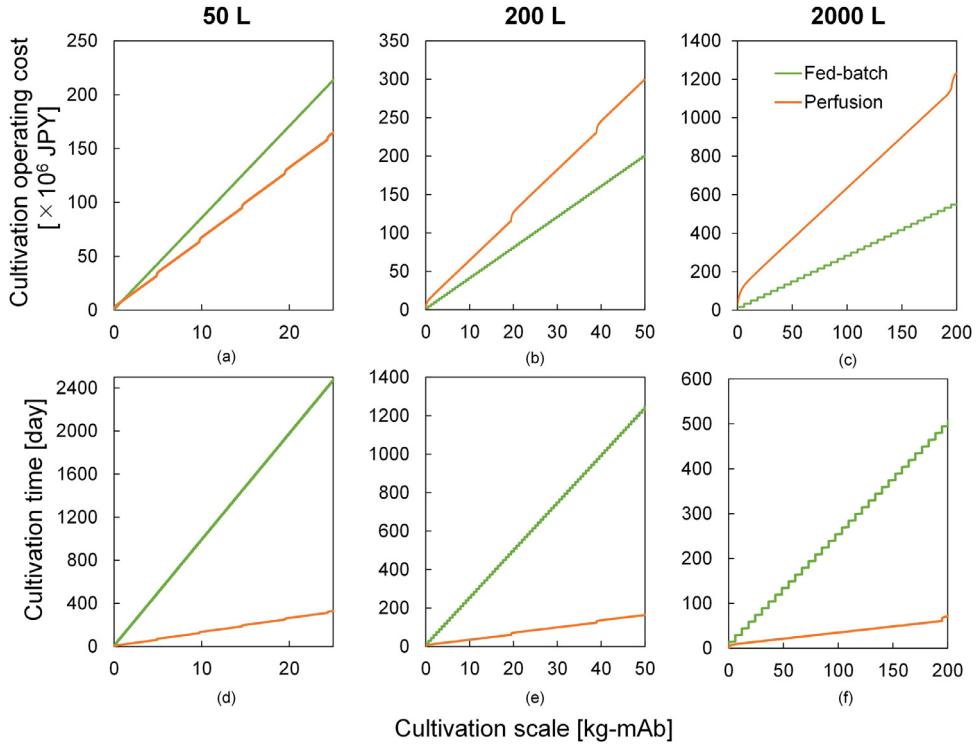

Fig. 7. Comparison of production (a-c) cost and (d-f) time between fed-batch and perfusion operations at different reactor volumes and mAb production scales.

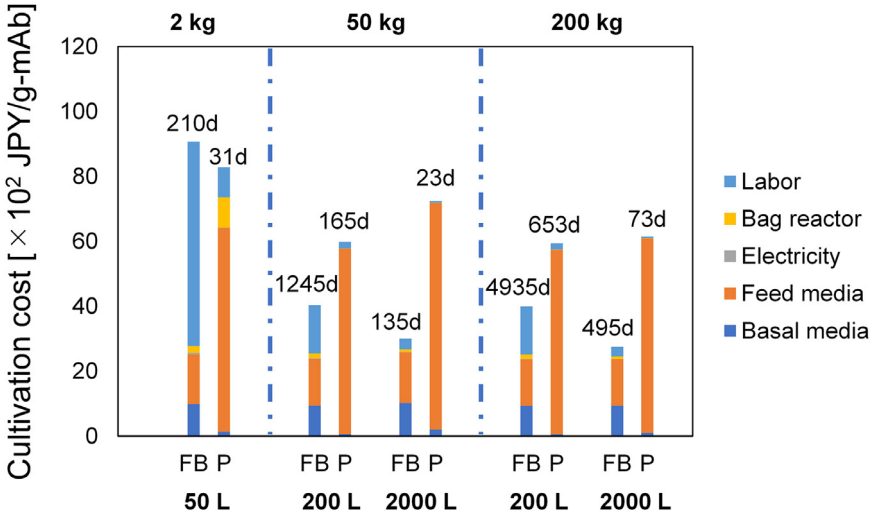

Fig. 8. Break down of cultivation cost per gram mAb of fed-batch (left) and perfusion (right) reactors for different production amounts and reactor volumes. The required operating time assuming one available reactor is indicated for each scenario.

ing that, while cultivation costs were dominant in the results of this analysis of operating costs, the calculation of total investment costs could feature downstream costs more heavily as they would include additional more expensive filters and equipment among other items. The sensitivity of the cost results to model assumptions should also be further investigated. The analysis was based on optimized conditions from pilot-scale operations adjusted for minimizing product losses and maximizing equipment use. For example, the maximum number of cycles for resin use (taken here as 200), could be lower (in the range of 100), which would lead to significant rises in resin costs. Switching between capture columns was taken at a conservative value of 30% breakthrough. Operating at nearly 100% breakthrough is possible, but could be more vulnerable to disturbances upstream, which could lead to significant product losses and the associated increase in costs. Optimal operation should thus balance robustness with production efficiency. Perfusion was shown to incur more operating costs in this analysis. However, it is still important to consider that this simulation does not account for the heating, ventilation, and air conditioning (HVAC) system costs. Perfusion operations with its smaller reactors would occupy a smaller production area and therefore incur lower HVAC costs. The smaller perfusion reactors and higher productivities also enable much higher production capacities and flexibility for plants with multiple products. Therefore, decision-makers could choose to prioritize having lower production times than costs in such cases.

Different decisions could be reached at each production stage. For example, prioritizing cost reduction at clinical manufacturing could have significant impacts in the R&D phase. Clinical manufacturing represents a significant portion of the non-clinical R&D

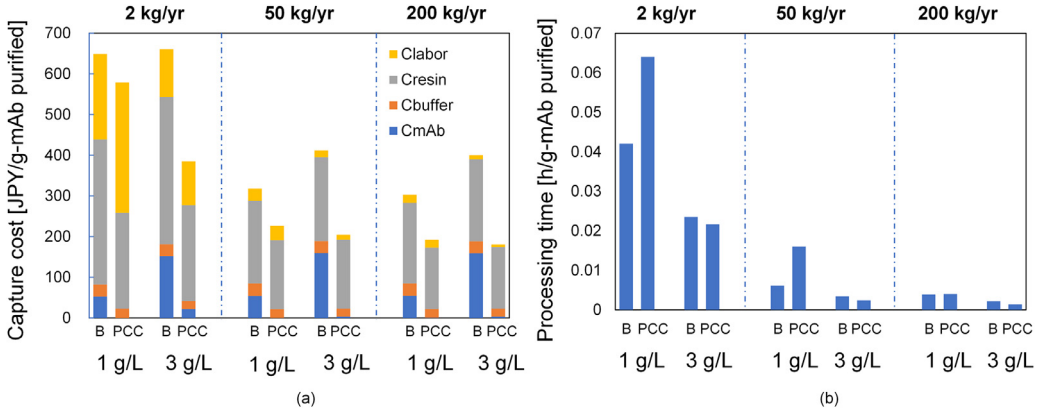

Fig. 9. Comparison of production (a) cost and (b) time per gram of mAb purified between batch (B on the left) and 3-column PCC (PCC on the right) at different annual production scales and inlet titers.

Table 5
Simulation results for integrated unit operations for mAb production within 200 working days at different manufacturing scales. FB= Fed-batch, *P*=Perfusion, *B*= Batch capture, PCC= Continuous capture.

ID	Annual production scale [kg-mAb/yr]	Reactor size [L]	No. of reactors	Average Titer [g/L]	Capture time [h]	Total operating cost [JPY]
FB-B	2	51	1	3.04	48	1.83E+07
FB-PCC					43	1.77E+07
P-B		7	1	1.77	61	2.39E+07
P-PCC					149*	2.40E+07
FB-B	50	1264	1	3.04	165	1.66E+08
FB-PCC					118	1.56E+08
P-B		169	1	1.74	217	3.22E+08
P-PCC					4254**	3.33E+08
FB-B	200	1686	3	3.04	419	6.37E+08
FB-PCC					263	5.96E+08
P-B		675	1	1.74	552	1.26E+09
P-PCC					4254**	1.24E+09

* 35 L surge tank available following perfusion operations for 5 days pooling time.
** operation in parallel to perfusion operations.

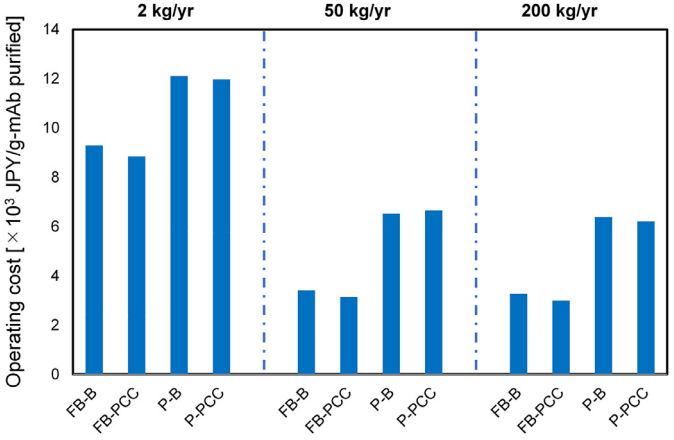

Fig. 10. Operating cost per gram mAb produced for integrated batch (FB-B), continuous (P-B), and hybrid scenarios (FB-PCC and P-B) of the cultivation and capture units at different annual production scales.

costs, which in turn, account for 20–30% of the total R&D costs (Pollock et al., 2017). While in the commercial production phase, increasing production capacity, flexibility, and efficiency could lead to prioritizing alternatives with lower production time. In this work, a perfusion titer of ≈1.75 g/L was achieved. Ongoing developments in perfusion operations could lead to higher titers (3–5 g/L), which could further tip the balance in favor of perfusion operations in terms of productivity.

Other factors should also be taken into consideration for the final assessment. For example, the costs of risk mitigation measures should also be accounted for. One such measure is the addition of intermediate surge tanks to smooth operations, as in hybrid operations, or where different flowrates are required for continuous operation in different units. For example, a surge tank was required in the case of the 2 kg/yr continuous scenario, where the capture rate would have been higher than the perfusion rate. Surge tanks could also serve as intermediate reserves in the case of operational difficulties in terms of partial failures and delays. Examples of such difficulties could include clogging in the case of perfusion operations or valve reliability issues in the chromatography unit. The cost of surge tanks has not been accounted for in this analysis. For normal operation, batch processes would require more tanks for storage between units. However, the expected operational difficulties with continuous operations might also require additional storage tanks as contingencies. More analysis of the expected failure rates and the sizes of the required tanks is required for a fair comparison between the different modes. The use of single-use equipment would also introduce supply risks necessitating appropriate levels of equipment storage to avoid disruptions in case of emergencies. The storage levels should be decided as a balance of costs and other elements such as maintaining equipment sterility. The effectiveness of downstream operations in removing leachables from single-use equipment has been shown in literature (Paudel et al., 2020), thus deeming the risk of compromising product quality as minimal (Zürcher et al., 2020).

Product quality is another important aspect that should be considered early in the process design phase. The model presented

in this work could serve as the basis where modules are added for product quality attributes, such HCPs and charge variant profiles. The ability to model propagating impacts of upstream units on downstream operations would facilitate the decision-making process. Different cultivation modes could lead to variations in the product quality attributes and could lead to complications in downstream purification operations (Badr and Sugiyama, 2020). A unified measure of quality in upstream and downstream operations is thus needed for integrated process design. These aspects should also be taken into consideration at the product registration stage, especially if different cultivation modes are chosen for clinical and commercial phases (Bielser et al., 2019).

4. Conclusions

This work compared batch, hybrid, and continuous operations in the main cultivation and capture chromatography units using single-use equipment with limited reactor sizes. A modified kinetic model was presented for the main cultivation unit. The model was validated using pilot and lab scale experiments from literature and from a pilot facility in Japan. The model was validated for product quantification using different cell lines and operating conditions. The assessment was conducted for individual and integrated scenarios at different production scales in terms of operating time and costs. Continuous operations of integrated units were shown as clearly superior in terms of productivity, albeit at higher costs compared to batch. Hybrid alternatives, with fed-batch cultivation and PCC capture, incurred the lowest operating costs per gram across all production scales.

Future work could include the extension of the assessment to other cultivation modes, such as concentrated fed-batch, or investigating the impacts of potential developments leading to higher titer perfusion. More unit operations could be included in the analysis. Further model developments could include improving the depiction of different cell phases and metabolic pathways as a function of operating conditions such as pH and temperature. A fairer and more comprehensive comparison of the alternatives could be carried out by including the impacts and probabilities of operational difficulties. The dynamic nature of the model employed in this work could facilitate such extensions of the assessment scope. The assessment could also be extended to include environmental impacts and product quality aspects.

The presented model could be further used to map out and characterize the design space for mAb manufacturing. It could also be used as the basis for the development of process design, control, and scheduling efforts. This could be carried out under a broader assessment framework aiming at reducing the overall costs and environmental impacts, in addition to social aspects such as the time to reach target patients. Achieving these goals would thus work towards improving the sustainability of biopharmaceutical manufacturing.

List of variables

ε_c	Column porosity
ε_p	Particle porosity
μ	Cell growth rate
μ_d	Cell death rate
μ_{max}	Maximum cell growth rate
c	Concentration in the bulk liquid phase
c_{Feed}	Feed concentration
c_{in}	Glucose concentration in the main feed
c_{inlet}	Column inlet concentration
c_p	Intra-particle liquid phase concentration
c_{suppl}	Glucose concentration in the supplementary feed
k_{Ai}	Adsorption rate constant at i^{th} adsorption site
k_d	Maximum cell death rate
k_f	Film mass transfer coefficient
k_s	Solid mass transfer coefficient
k_{tot}	Total mass transfer coefficient
m_{glc}	Glucose maintenance coefficient
m_{loaded}	Mass of mAb loaded to the chromatography unit
$m_{purified}$	Mass of purified mAb obtained from the chromatography unit
n_{col}	Number of chromatography columns
n_{cycle}	Number of chromatography cycles needed to treat all input from cultivation in one year
n_{life}	Maximum number of load/regeneration cycles within resin lifespan
q_i	Solid phase concentration on i^{th} adsorption site
q^{sat}	Resin saturation capacity
r_p	Particle radius
$t_{1\%}$	Time for 1% breakthrough
$t_{changeover}$	Changeover time between runs
t_{demand}	Duration of last perfusion run if a fraction of a run is needed to fulfill demand
t_{empty}	Time to empty the reactor after the feed stops in perfusion runs.
$t_{fed-batch}$	Time to complete one fed-batch run
t_i	Duration of each column regeneration step i, including wash, elution, cleaning in place, and equilibration
t_{load}	Column loading time
$t_{perfusion}$	Time to complete one perfusion run
$t_{PLW,max}$	Maximum post load wash duration
t_{switch}	Phase duration within a PCC cycle
$t_{total,\ mode}$	Total time to fulfill production demand in fed-batch or perfusion modes
u_{sf}	Superficial velocity
$u_{sf,regen}$	Superficial velocity during column regeneration
x	Distance travelled along column length
C_i	Cost of item i
D_L	Axial dispersion coefficient
F_{bleed}	Bleed flow rate
$F_{harvest}$	Harvest flow rate
F_{in}	Main feed flow rate
F_{suppl}	Supplementary feed flow rate
$[GLC]$	Glucose concentration
K_D	Equilibrium constant
KD_{glc}	Half maximum death rate glucose concentration
KD_{lac}	Half maximum death rate lactate concentration
K_{glc}	Half maximum growth rate glucose concentration
KI_{lac}	Half maximum growth rate lactate concentration
$[LAC]$	Lactate concentration
$N_{operator}$	Number of operators
N_{run}	Number of runs to fulfill production demand.
P	Antibody product concentration
P_i	Unit Price of item i (Table 2)
Q	Flow rate in loading the chromatography column
Q_P	Antibody specific production rate
S	Column surface area
V	Culture Volume
V_{col}	Volume of chromatography columns
V_{cult}	Total cultivation volume to be treated
V_i	Buffer volume used in each regeneration step i, including wash, elution, cleaning in place, and equilibration
V_r	Reactor volume
V_{r_ref}	Reference reactor volume
X_V	Viable cell density
$Y_{lac/glc}$	Yield coefficient (change in lactate with variations in glucose)
Y_{resin}	Resin lifespan
$Y_{X_V/glc}$	Yield coefficient (change in cell density with variations in glucose)

Author statement

Sara Badr: Conceptualization, Methodology, Formal analysis, Validation, Writing-original draft, Writing- Review & editing, Visualization, Supervision.

Kozue Okamura: Conceptualization, Methodology, Software, Validation, Data Curation, Formal analysis, Writing-Review & editing.

Nozomi Takahashi: Conceptualization, Methodology, Software, Validation, Data Curation, Formal analysis, Writing-Review & editing.

Vera Ubbenjans: Conceptualization, Methodology, Software.

Haruku Shirahata: Conceptualization, Methodology.

Hirokazu Sugiyama: Conceptualization, Methodology, Writing-Review & editing, Formal analysis, Resources, Supervision, Project administration, Funding acquisition.

Declaration of Competing Interest

The authors declare no conflicts of interest associated with this manuscript.

Acknowledgements

This work was supported by the Japan Agency for Medical Research and Development (AMED) [grant No. JP19ae0101064, JP19ae0101058, JP17ae0101003]. Experimental data from the Kobe GMP consolidated lab of Manufacturing Technology Association of Biologics is gratefully acknowledged. The help and insights from Prof. Takeshi Omasa (Osaka University), Prof. Yamamoto (Yamaguchi University), and Dr. Sei Murakami and Mr. Kazuo Kobayashi (Manufacturing Technology Association of Biologics) are also gratefully acknowledged.

Supplementary materials

Supplementary material associated with this article can be found, in the online version, at doi:10.1016/j.compchemeng.2021.107422.

References

Badr, S., Okamura, K., Takahashi, N., Ubbenjans, V., Shirahata, H., Sugiyama, H., 2020. Integrated Design of Biopharmaceutical Manufacturing Processes: operation Modes and Process Configurations for Monoclonal Antibody Production, in: Computer Aided Chemical Engineering. https://doi.org/10.1016/B978-0-12-823377-1.50269-X

Badr, S., Sugiyama, H., 2020. A PSE perspective for the efficient production of monoclonal antibodies: integration of process, cell, and product design aspects. Curr. Opin. Chem. Eng. 27, 121–128. doi:10.1016/j.coche.2020.01.003.

Baumann, P., Hubbuch, J., 2017. Downstream process development strategies for effective bioprocesses: trends, progress, and combinatorial approaches. Eng. Life Sci. 17, 1142–1158. doi:10.1002/elsc.201600033.

Baur, D., Angarita, M., Müller-Späth, T., Steinebach, F., Morbidelli, M., 2016. Comparison of batch and continuous multi-column protein A capture processes by optimal design. Biotechnol. J. 11, 920–931. doi:10.1002/biot.201500481.

Bielser, J.M., Chappuis, L., Xiao, Y., Souquet, J., Broly, H., Morbidelli, M., 2019. Perfusion cell culture for the production of conjugated recombinant fusion proteins reduces clipping and quality heterogeneity compared to batch-mode processes. J. Biotechnol. 302, 26–31. doi:10.1016/j.jbiotec.2019.06.006.

Bunnak, P., Allmendinger, R., Ramasamy, S.V., Lettieri, P., Titchener-Hooker, N.J., 2016. Life-cycle and cost of goods assessment of fed-batch and perfusion-based manufacturing processes for mAbs. Biotechnol. Prog. 32, 1324–1335. doi:10.1002/btpr.2323.

Cataldo, A.L., Burgstaller, D., Hribar, G., Jungbauer, A., Satzer, P., 2020. Economics and ecology: modelling of continuous primary recovery and capture scenarios for recombinant antibody production. J. Biotechnol. 308, 87–95. doi:10.1016/j.jbiotec.2019.12.001.

Croughan, M.S., Konstantinov, K.B., Cooney, C., 2015. The future of industrial bioprocessing: batch or continuous? Biotechnol. Bioeng. 112, 648–651. doi:10.1002/bit.25529.

Fisher, A.C., Kamga, M.H., Agarabi, C., Brorson, K., Lee, S.L., Yoon, S., 2019. The Current Scientific and Regulatory Landscape in Advancing Integrated Continuous Biopharmaceutical Manufacturing. Trends Biotechnol 37, 253–267. doi:10.1016/j.tibtech.2018.08.008.

Godawat, R., Konstantinov, K., Rohani, M., Warikoo, V., 2015. End-to-end integrated fully continuous production of recombinant monoclonal antibodies. J. Biotechnol. 213, 13–19. doi:10.1016/j.jbiotec.2015.06.393.

Grilo, A.L., Mantalaris, A., 2019. The Increasingly Human and Profitable Monoclonal Antibody Market. Trends Biotechnol. 37, 9–16. doi:10.1016/j.tibtech.2018.05.014.

Hong, M.S., Severson, K.A., Jiang, M., Lu, A.E., Love, J.C., Braatz, R.D., 2018. Challenges and opportunities in biopharmaceutical manufacturing control. Comput. Chem. Eng. 110, 106–114. doi:10.1016/j.compchemeng.2017.12.007.

Karst, D.J., Steinebach, F., Morbidelli, M., 2018. Continuous integrated manufacturing of therapeutic proteins. Curr. Opin. Biotechnol. 53, 76–84. doi:10.1016/j.copbio.2017.12.015.

Kesik-Brodacka, M., 2018. Progress in biopharmaceutical development. Biotechnol. Appl. Biochem. 65, 306–322. doi:10.1002/bab.1617.

Klutz, S., Holtmann, L., Lobedann, M., Schembecker, G., 2016. Cost evaluation of antibody production processes in different operation modes. Chem. Eng. Sci. 141, 63–74. doi:10.1016/j.ces.2015.10.029.

Kornecki, M., Strube, J., 2018. Process analytical technology for advanced process control in biologics manufacturing with the aid of macroscopic kinetic modeling. Bioengineering 5. doi:10.3390/bioengineering5010025.

Lalor, F., Fitzpatrick, J., Sage, C., Byrne, E., 2019. Sustainability in the biopharmaceutical industry: seeking a holistic perspective. Biotechnol. Adv. 37, 698–707. doi:10.1016/j.biotechadv.2019.03.015.

Lin, H., Leighty, R.W., Godfrey, S., Wang, S.B., 2017. Principles and approach to developing mammalian cell culture media for high cell density perfusion process leveraging established fed-batch media. Biotechnol. Prog. 33, 891–901. doi:10.1002/btpr.2472.

Moorkens, E., Meuwissen, N., Huys, I., Declerck, P., Vulto, A.G., Simoens, S., 2017. The market of biopharmaceutical medicines: a snapshot of a diverse industrial landscape. Front. Pharmacol. 8. doi:10.3389/fphar.2017.00314.

Papathanasiou, M.M., Kontoravdi, C., 2020. Engineering challenges in therapeutic protein product and process design. Curr. Opin. Chem. Eng. 27, 81–88. doi:10.1016/j.coche.2019.11.010.

Paudel, K., Hauk, A., Maier, T.V., Menzel, R., 2020. Quantitative characterization of leachables sinks in biopharmaceutical downstream processing. Eur. J. Pharm. Sci. 143, 105069. doi:10.1016/j.ejps.2019.105069.

Pleitt, K., Somasundaram, B., Johnson, B., Shave, E., Lua, L.H.L., 2019. Evaluation of process simulation as a decisional tool for biopharmaceutical contract development and manufacturing organizations. Biochem. Eng. J. 150, 107252. doi:10.1016/j.bej.2019.107252.

Pollock, J., Bolton, G., Coffman, J., Ho, S.V., Bracewell, D.G., Farid, S.S., 2013a. Optimising the design and operation of semi-continuous affinity chromatography for clinical and commercial manufacture. J. Chromatogr. A 1284, 17–27. doi:10.1016/j.chroma.2013.01.082.

Pollock, J., Coffman, J., Ho, S.V., Farid, S.S., 2017. Integrated continuous bioprocessing: economic, operational, and environmental feasibility for clinical and commercial antibody manufacture. Biotechnol. Prog. 33, 854–866. doi:10.1002/btpr.2492.

Pollock, J., Ho, S.V., Farid, S.S., 2013b. Fed-batch and perfusion culture processes: economic, environmental, and operational feasibility under uncertainty. Biotechnol. Bioeng. 110, 206–219. doi:10.1002/bit.24608.

Radhakrishnan, D., Wells, E.A., Robinson, A.S., 2018. Strategies to enhance productivity and modify product quality in therapeutic proteins. Curr. Opin. Chem. Eng. 22, 81–88. doi:10.1016/j.coche.2018.09.005.

Rathore, A.S., Kateja, N., Kumar, D., 2018. Process integration and control in continuous bioprocessing. Curr. Opin. Chem. Eng. 22, 18–25. doi:10.1016/j.coche.2018.08.005.

Seymour, P., Ecker, D.M., 2017. Global Biomanufacturing Trends, Capacity, and Technology Drivers: industry Biomanufacturing Capacity Overview [WWW Document]. URL https://www.americanpharmaceuticalreview.com/Featured-Articles/188840-Global-Biomanufacturing-Trends-Capacity-and-Technology-Drivers-Industry-Biomanufacturing-Capacity-Overview/

Sha, S., Huang, Z., Wang, Z., Yoon, S., 2018. Mechanistic modeling and applications for CHO cell culture development and production. Curr. Opin. Chem. Eng. 22, 54–61. doi:10.1016/j.coche.2018.08.010.

Shirahata, H., Badr, S., Dakessian, S., Sugiyama, H., 2019a. Alternative generation and multiobjective evaluation using a design framework: case study on sterile filling processes of biopharmaceuticals. Comput. Chem. Eng. 123. doi:10.1016/j.compchemeng.2018.12.019.

Shirahata, H., Diab, S., Sugiyama, H., Gerogiorgis, D.I., 2019b. Dynamic modelling, simulation and economic evaluation of two CHO cell-based production modes towards developing biopharmaceutical manufacturing processes. Chem. Eng. Res. Des. 150, 218–233. doi:10.1016/j.cherd.2019.07.016.

Steinebach, F., Angarita, M., Karst, D.J., Müller-Späth, T., Morbidelli, M., 2016. Model based adaptive control of a continuous capture process for monoclonal antibodies production. J. Chromatogr. A 1444, 50–56. doi:10.1016/j.chroma.2016.03.014.

von Lieres, E., Andersson, J., 2010. A fast and accurate solver for the general rate model of column liquid chromatography. Comput. Chem. Eng. 34, 1180–1191. doi:10.1016/j.compchemeng.2010.03.008.

Walsh, G., 2018. Biopharmaceutical benchmarks 2018. Nat. Biotechnol. 36, 1136–1145. doi:10.1038/nbt.4305.

Walther, J., Lu, J., Hollenbach, M., Yu, M., Hwang, C., McLarty, J., Brower, K., 2019. Perfusion Cell Culture Decreases Process and Product Heterogeneity in a Head-to-Head Comparison With Fed-Batch. Biotechnol. J. 14, 1–10. doi:10.1002/biot.201700733.

Warikoo, V., Godawat, R., Brower, K., Jain, S., Cummings, D., Simons, E., Johnson, T., Walther, J., Yu, M., Wright, B., Mclarty, J., Karey, K.P., Hwang, C., Zhou, W., Riske, F., Konstantinov, K., 2012. Integrated Continuous Production of Recombinant Therapeutic Proteins 109, 3018–3029. https://doi.org/10.1002/bit.24584

Xing, Z., Bishop, N., Leister, K., Li, Z.J., 2010. Modeling kinetics of a large-scale fed-batch CHO cell culture by markov chain monte carlo method. Biotechnol. Prog. 26, 208–219. doi:10.1002/btpr.284.

Xu, S., Chen, H., 2016. High-density mammalian cell cultures in stirred-tank bioreactor without external pH control. J. Biotechnol. 231, 149–159. doi:10.1016/j.jbiotec.2016.06.019.

Xu, S., Gavin, J., Jiang, R., Chen, H., 2017. Bioreactor productivity and media cost comparison for different intensified cell culture processes. Biotechnol. Prog. 33, 867–878. doi:10.1002/btpr.2415.

Yang, O., Prabhu, S., Ierapetritou, M.G., 2019a. A Comparison Between Batch and Continuous Monoclonal Antibody Production and Economic Analysis. Ind. Eng. Chem. Res. doi:10.1021/acs.iecr.8b04717.

Yang, O., Qadan, M., Ierapetritou, M., 2019b. Economic Analysis of Batch and Continuous Biopharmaceutical Antibody Production: a Review. J. Pharm. Innov. doi:10.1007/s12247-018-09370-4.

Zhang, Y., Stobbe, P., Silvander, C.O., Chotteau, V., 2015. Very high cell density perfusion of CHO cells anchored in a non-woven matrix-based bioreactor. J. Biotechnol. 213, 28–41. doi:10.1016/j.jbiotec.2015.07.006.

Zürcher, P., Shirahata, H., Badr, S., Sugiyama, H., 2020. Multi-stage and multi-objective decision-support tool for biopharmaceutical drug product manufacturing: equipment technology evaluation. Chem. Eng. Res. Des. 161. doi:10.1016/j.cherd.2020.07.004.

Zydney, A.L., 2016. Continuous downstream processing for high value biological products: a Review. Biotechnol. Bioeng. 113, 465–475. doi:10.1002/bit.25695.